



Innovative superparamagnetic iron-oxide nanoparticles coated with silica and conjugated with linoleic acid: Effect on tumor cell growth and viability



Giuliana Muzio^a, Marta Miola^{b,d,1}, Sara Ferraris^{b,1}, Marina Maggiora^a, Elisa Bertone^b, Maria Paola Puccinelli^c, Marina Ricci^a, Ester Borroni^d, Rosa Angela Canuto^{a,1}, Enrica Verné^{b,*,1}, Antonia Follenzi^{d,*,*,1}

^a Department of Clinical and Biological Sciences, University of Turin, Corso Raffaello 30, 10125 Turin, Italy

^b Department of Applied Science and Technology, Politecnico di Torino, Corso Duca degli Abruzzi 24, 10129 Turin, Italy

^c Department of Laboratory Medicine, Azienda Ospedaliera Universitaria, Città della Salute e della Scienza, Corso Bramante 88/90, 10126 Turin, Italy

^d Department of Health Sciences, University "Amedeo Avogadro" of East Piedmont, Novara, Italy

ARTICLE INFO

Article history:

Received 18 October 2016

Received in revised form 14 February 2017

Accepted 9 March 2017

Available online 10 March 2017

ABSTRACT

One of the goals for the development of more effective cancer therapies with reduced toxic side effects is the optimization of innovative treatments to selectively kill tumor cells. The use of nanovectors loaded with targeted therapeutic payloads is one of the most investigated strategies. In this paper superparamagnetic iron oxide nanoparticles (SPIONs) coated by a silica shell or uncoated, were functionalized with single-layer and bi-layer conjugated linoleic acid (CLA). Silica was used to protect the magnetic core from oxidation, improve the stability of SPIONs and tailor their surface reactivity. CLA was used as novel grafting biomolecule for its anti-tumor activity and to improve particle dispersibility. Mouse breast cancer 4T1 cells were treated with these different SPIONs. SPIONs functionalized with the highest quantity of CLA and coated with silica shell were the most dispersed. Cell viability was reduced by SPIONs functionalized with CLA in comparison with cells which were untreated or treated with SPIONs without CLA. As regards the types of SPIONs functionalized with CLA, the lowest viability was observed in cells treated with uncoated SPIONs with the highest quantity of CLA.

In conclusion, the silica shell free SPIONs functionalized with the highest amount of CLA can be suggested as therapeutic carriers because they have the best dispersion and ability to decrease 4T1 cell viability.

© 2017 Elsevier B.V. All rights reserved.

1. Introduction

Some progress has been made in the field of anticancer therapies, although the research on new strategies to find even more effective therapies and to reduce their toxic side effects is still needed. The development of innovative treatments to kill tumor or metastatic cells is a challenging goal and for this reason, several possible approaches are under investigation. Today nanomedicine-based therapies are used in cancer research because they can bypass cancer cell multi-drug resistance, poor solubility of hydrophobic anti-cancer drugs, and the use of

dangerous radiations [1]. Cancer nanomedicine pays particular attention to superparamagnetic iron oxide nanoparticles (SPIONs), that can reach the tumor sites carrying chemotherapeutic drugs, nucleic acids, monoclonal antibodies, viral vectors engineered with therapeutic suicide genes or shRNAs [1,2,3]. SPIONs are also used for diagnostic assays, generation of local hyperthermia for tumor therapy or tissue repair by delivering stem cells [4,5]. In fact, SPIONs can be combined with contrast fluorescent agents to improve cancer cell imaging [1]. In hyperthermia therapy, SPIONs are localized near the cancer site by magnetic driving and can induce localized heating by an external alternating magnetic field. For example in “in vitro” experiments, 14 nm magnetic nanoclusters killed about 74% of MCF-7 cancer cells, by applying temperature of 45 °C for 1 h [6]. Similarly, a temperature of 43 °C for about 17 min reduced the viability of HeLa cells exposed to an alternating magnetic field in the presence of silica coated iron oxide nanoparticles (NPs) [7]. SPIONs can be internalized in human mesenchymal stem cells without affecting viability and structure. Following this, the SPION-loaded stem cells can be attracted to specific sites by applying an external magnetic field [8].

* Corresponding author.

** Correspondence to: A. Follenzi, Department of Health Sciences, University "Amedeo Avogadro" of East Piedmont, Via Solaroli 17, 28100 Novara, Italy.

E-mail addresses: giuliana.muzio@unito.it (G. Muzio), marta.miola@polito.it (M. Miola), sara.ferraris@polito.it (S. Ferraris), marina.maggiora@unito.it (M. Maggiora), elisa.bertone@polito.it (E. Bertone), mpuccinelli@cittadellasalute.to.it (M.P. Puccinelli), marina.ricci@unito.it (M. Ricci), rosangela.canuto@unito.it (R.A. Canuto), enrica.verne@polito.it (E. Verné), antonia.follenzi@med.uniupo.it (A. Follenzi).

¹ Co-shared authorship.

When preparing SPIONs for the delivery of chemotherapeutic agents it is important to control their size, shape and surface properties, in order to assure their stability in solution and maintain superparamagnetic properties also in the presence of a variety of molecules. SPIONs which are smaller than 100 nm can easily circulate in the blood without being captured by reticulo-endothelial cells and can therefore selectively accumulate in the tumor microenvironment [3]. On the contrary unmodified SPIONs tend to aggregate into large clusters and several studies suggest surface modification to avoid NP aggregation. A widely explored solution is surface coverage by polymers that has the unavoidable disadvantage of causing an increase in particle size and a potential loss in magnetic response [1]. Alternatively, small intermediary molecules can be used, acting as stabilizing agents and for the subsequent coupling of functional molecules. Fatty acids, in particular oleic acid (OA), have been used as capping agent to obtain monodisperse SPIONs suspensions [9].

This study aimed to prepare functionalized SPIONs able to affect tumor cell viability. SPIONs, either coated with silica shell or uncoated, were prepared and functionalized with conjugated linoleic acid (CLA) in single- and bi-layer configuration. Silica was used for its ability to protect the magnetic core from oxidation, to improve the magnetite stability and to tailor the surface reactivity by improving biomolecule grafting [10]. CLA was chosen to improve SPION dispersion and to add an anti-cancer potential [11–13]. Fatty acids are crucial structural and functional cell components, and contribute to the functional/physical/chemical features of membranes [11–13]. Concerning cancer, it is well known that carcinogenesis is characterized by changes in fatty acid composition of membrane phospholipids.

2. Materials and methods

2.1. Synthesis of superparamagnetic iron-oxide nanoparticles (Fe_3O_4)

Among the different methods for the SPIONs production, the co-precipitation process was selected since it is simple, rapid and allows a high yield. An aqueous solution of Fe^{2+} and Fe^{3+} salts in a 1:2 M ratio was prepared by mixing $FeCl_2 \cdot 4H_2O$ and $FeCl_3 \cdot 6H_2O$ in bi-distilled water; subsequently the mixture was mechanically mixed at 300 rpm and Fe_3O_4 precipitation occurred by adding NH_4OH drop by drop, until the pH of the mixture reached about 10. The suspension was put in ultrasound for 20 min; subsequently an aliquot was washed twice with bi-distilled water to remove the unreacted reagents (Fe_3O_4), while the other aliquot was not washed (Fe_3O_4 -NW).

2.2. One-step synthesis of conjugated linoleic acid-capped Fe_3O_4

In this procedure conjugated linoleic acid (CLA) was added in a single-step to the NP suspensions. A first synthesis of CLA-capped Fe_3O_4 NPs was carried out by adding drop by drop 3.0 μ l of CLA/ml of NP suspension, to both washed (Fe_3O_4 + CLA1) or not washed (Fe_3O_4 -NW + CLA1), NP under mechanical mixing. A second synthesis (Fe_3O_4 + CLA2) was performed using a higher amount of CLA (4.5 μ l CLA/ml of NPs suspension). All suspensions were heated at 80 °C with stirring at 150 rpm for half hour. At the end of the functionalization process NP suspensions were washed twice with ethanol and re-suspended in bi-distilled water.

2.3. Two-step synthesis of conjugated linoleic acid-capped Fe_3O_4

In this procedure CLA was added in two steps to the NP suspensions. The two-step CLA-capped Fe_3O_4 NPs were synthesized by adding, in a second step, a further aliquot of CLA (3.0 μ l CLA/ml of NP suspension) in the suspension of the one-step CLA-coated Fe_3O_4 NPs, both washed (Fe_3O_4 + CLA1-TS) and not washed (Fe_3O_4 -NW + CLA1-TS). The suspension was placed in orbital shaker at 80 °C at 150 rpm for half hour. Subsequently, NPs were washed twice with ethanol and re-suspended

in bi-distilled water, adjusting the pH at 12 by adding NH_4OH drop by drop [14].

2.4. Synthesis of silica-coated magnetite nanoparticles (Fe_3O_4 - SiO_2)

In order to promote the single nanoparticles coating in a uniform way and obtain a stable suspension, Fe_3O_4 NPs were stabilized with 0.05 M citric acid. The pH was adjusted to 5.2 by dropwise NH_4OH and the suspension was placed 90 min at room temperature in orbital shaker (KS 4000i control, IKA®) at 150 rpm allowing the deprotonation of two carboxylic groups of citric acid and the bond to the OH groups exposed by Fe_3O_4 NPs [15]. Subsequently, citric acid-functionalized NPs were washed with bi-distilled water using an ultrafiltration device (Solvent Resistant Stirred Cells - Merck Millipore) and re-suspended in bi-distilled water, adjusting the pH at about 10.1 to induce the deprotonation of the third carboxylic group, which allow an optimal NP dispersion. Then, magnetite NPs functionalized with citric acid were coated with a silica shell (Fe_3O_4 - SiO_2) by sol-gel method, by adding TEOS (tetraethoxysilane) as silica precursor, ethanol as catalyst and water as solvent, to Fe_3O_4 NPs suspended in a water and ethanol solution (water: ethanol 1:4) [16]. The pH of suspension was adjusted at 10 (NH_4OH); the suspension was placed in orbital shaker at room temperature for 3 h at 150 rpm. Subsequently, the Fe_3O_4 - SiO_2 NPs were washed with bi-distilled water using an ultrafiltration device (Solvent Resistant Stirred Cells - Merck Millipore) and re-dispersed in water.

2.5. One-step synthesis of conjugated linoleic acid-capped Fe_3O_4 - SiO_2

On the base of the results obtained for CLA coated Fe_3O_4 , Fe_3O_4 - SiO_2 were functionalized with the higher CLA amount (4.5 μ l CLA/ml of NPs) with one-step procedure (Fe_3O_4 - SiO_2 + CLA2). The suspension was heated at 80 °C and stirred at 150 rpm for half hour. At the end of the functionalization process CLA capped Fe_3O_4 - SiO_2 NPs were washed twice with ethanol and re-suspended in bi-distilled water.

Table 1 resumes the name and samples composition. All chemicals were purchased from Sigma-Aldrich Co. (St Louis, MO, USA).

2.6. Nanoparticles characterization

All synthesized NPs were subjected to morphological characterization by scanning transmission electron microscopy (STEM, MERLIN Zeiss – Germany). For STEM observation, a drop of diluted NP suspension was deposited on a copper TEM grid with carbon film (SPI Supplies® Brand Lacey Carbon Coated 200 Mesh Copper Grids – JEOL S.p.A.). Fourier transformation infrared spectroscopy (FT-IR) was used to evidence the effective grafting of CLA and to confirm the presence of silica shell. FT-IR spectra were acquired in a Hyperion 2000 FT/IR (Tensor 27, Bruker Optics S.p.A, Ettlingen, Germany) from 4000 to 400 cm^{-1} and with 2 cm^{-1} resolution. OPUS software (v. 6.5, Bruker S.p.A) was used for instrumental control and spectral acquisition. Suspension stability and dispersion were evaluated in a semi-quantitative way by measuring the time required for particle precipitation.

Table 1
Name and composition of the samples.

Acronym	NPs	Washing	CLA	CLA [μ l] per 1 ml of NPs suspension
Fe_3O_4 + CLA1	Fe_3O_4	Yes	one-step	3.0
Fe_3O_4 -NW + CLA1	Fe_3O_4	No	one-step	3.0
Fe_3O_4 + CLA1-TS	Fe_3O_4	Yes	two-step	3.0
Fe_3O_4 -NW + CLA1-TS	Fe_3O_4	No	two-step	3.0
Fe_3O_4 + CLA2	Fe_3O_4	Yes	one-step	4.5
Fe_3O_4 - SiO_2 + CLA2	Fe_3O_4 - SiO_2	Yes	one-step	4.5

2.7. Cell cultures: treatment of 4T1 with Fe₃O₄ NPs capped or not with CLA, or with CLA alone, and of MS1 cells with Fe₃O₄ NPs capped or not with CLA

Mouse breast cancer 4T1 cells were seeded (12,500 cells/cm²) in DMEM/F-12 medium supplemented with 2 mM glutamine, 1% (v/v) antibiotic/antimycotic solution, 10% (v/v) fetal bovine serum (FBS) and maintained at 37 °C in a humidified atmosphere of 5% CO₂ in air. Mouse pancreatic islet endothelial MS1 cells were seeded (12,500 cells/cm²) in DMEM medium supplemented with 1% glutamine, 1% (v/v) antibiotic solution, 10% (v/v) fetal bovine serum (FBS). Both cell lines were maintained at 37 °C in a humidified atmosphere of 5% CO₂ in air and 24 h after seeding, culture medium was removed and replaced by the same medium not supplemented or supplemented with Fe₃O₄, Fe₃O₄-SiO₂, Fe₃O₄ + CLA1, Fe₃O₄-NW + CLA1, Fe₃O₄ + CLA1-TS, Fe₃O₄-NW + CLA1-TS, Fe₃O₄ + CLA2 and Fe₃O₄-SiO₂ + CLA2 at the concentrations 8 µg or 16 µg of NPs/100,000 cells. Twenty-four hours after seeding, the 4T1 cells were also treated with CLA alone at 10 and 25 µM concentrations. The experimental times were 24, 48 and 72 h.

2.7.1. Cell viability

Cell viability was evaluated by means of the MTT assay after 24, 48 and 72 h of treatment. 4T1 or MS1 cells grown in multiwells were added with 30 µl of 4.5-dimethylthiazol-2-yl-,5-diphenyltetrazolium bromide (MTT, 5 mg/ml) in PBS solution, and incubated for 3 h at 37 °C in a humidified atmosphere of 5% CO₂ in air. After the supernatants were removed and 150 µl of DMSO was added to each well. After 20 min of incubation, the absorbance was measured at 590 nm using a microplate reader (Dynatech MR580 microElisa, USA).

2.7.2. Iron staining

After 24 and 72 h of treatment in chamber slides, the iron stain KIT HT20 (Sigma-Aldrich Co., St Louis, MO, USA) was used to evidence the SPIONs functionalized or not with CLA internalized by 4T1 and MS1 cells.

2.7.3. CLA percentage content in incubated cells

As indication of CLA-capped NP internalization, the CLA percentage content was determined in lipids extracted from 6 × 10⁶ cells previously incubated with Fe₃O₄, Fe₃O₄ + CLA1, Fe₃O₄ + CLA2 or Fe₃O₄-SiO₂ + CLA2 NPs for 72 h. After treatment, the cells were washed with PBS + EDTA (0.53 mM), detached with trypsin/EDTA (0.25%/0.3%), and centrifuged at 600 g for 10 min at 4 °C.

Lipids, isolated by Folch et al. method [17], were suspended in 0.5 ml of methanol containing internal standard 1,2-dihexanoyl-sn-glycero-phosphocholine. The method of Klem et al. [18] for analysis of red blood cell fatty acid composition was adapted for the determination of CLA in 4T1 cell lipids. The extracts were evaporated under nitrogen flow, dissolved with chilled methanol containing 2,6 di-ter-butyl-4-methyl-phenol (BHT) as antioxidant, treated for 15 min in an ultrasound bath and then centrifuged. The supernatants were treated with a methanol solution of sodium methoxide to synthesize CLA methyl esters, and after 5 min a hydrochloric acid solution was added. CLA methyl esters were extracted twice with hexane, evaporated under nitrogen flow at 35 °C, and re-dissolved in hexane containing BHT for injection in gas chromatograph–mass spectrometer. CLA were identified and quantified with a mass spectrometer operating in electron impact ionization (EI) mode. The selection of ions for selective ion monitoring (SIM) was based on comparison with standards and those reported in the literature [19,20].

2.8. Statistical analysis

All data are expressed as means ± SD. Differences between group means were assessed by analysis of variance followed by a post hoc Newman–Keuls test.

3. Results

3.1. Nanoparticles synthesis and characterization

The superparamagnetic properties and the XRD pattern of Fe₃O₄ NPs obtained with analogue procedure have been previously assessed [21]. Fig. 1 shows STEM analyses of Fe₃O₄ + CLA1, Fe₃O₄-NW + CLA1, Fe₃O₄ + CLA1-TS, Fe₃O₄-NW + CLA1-TS, Fe₃O₄ + CLA2 and Fe₃O₄-SiO₂ + CLA2 NPs. All NPs present a spherical shape with a dimensional range of about 5–15 nm, with the exception of silica coated NPs, seeming slightly bigger (up to 20 nm). A silica shell (of about 1–2 nm) is well visible in the micrograph (last panel of Fig. 1) and is evidenced by arrows.

FT-IR spectra of pure CLA, Fe₃O₄ + CLA1, Fe₃O₄-NW + CLA1, Fe₃O₄ + CLA1-TS, Fe₃O₄-NW + CLA1-TS are reported in Fig. 2. Fig. 2a shows the spectrum of CLA, in which two peaks at about 2852 e 2922 cm⁻¹ are assigned respectively to the asymmetric and symmetric stretching of CH₂; the peak at about 1710 cm⁻¹ can be attributed to the C=O stretch vibration, the peak at 1460 cm⁻¹ to the —COO⁻ asymmetric stretch vibration [14], the peak at 1408 to the “umbrella” bending mode of CH₃ group [14], the band between 1250 and 1285 cm⁻¹ can be associated to the presence of the C—O stretch or more generally to the vibration of the COOH group in oleic acid [22,23], the peaks at 981 and 945 cm⁻¹ are characteristic of the *cis,trans* conjugated dienes [24] and the peak at about 720 cm⁻¹ can be assigned both to CH₂ bending or rocking vibration and CH=CH vibration [24,23]. No significant differences can be observed in the FT-IR spectrum of pure CLA treated at 80 °C (not reported), as a confirmation that the functionalization procedure does not alter the molecule. Fig. 2b shows the whole spectrum for all NPs, showing peaks at about 560 cm⁻¹, ascribable to Fe—O stretching vibrational mode of Fe₃O₄, peaks at about 2852 e 2922 cm⁻¹ that can be assigned respectively to the asymmetric and symmetric stretching of CH₂ group of CLA, and a peak at about 1408 cm⁻¹ which can be ascribed to the “umbrella” bending mode of CH₃ group [14]. Focusing the analysis between 1000 and 4000 cm⁻¹ (Fig. 2c), it is possible to notice also the presence of a broad band at about 1500–1640 cm⁻¹ that can be attributed to the asymmetric and symmetric stretch vibration of COO⁻ group reported in literature for fatty acids adsorbed on Fe₃O₄ [14,22]. Moreover, in the Fe₃O₄ + CLA1-TS and Fe₃O₄-NW + CLA1-TS curves, the band at about 1250–1285 cm⁻¹ and the peak at about 1710 cm⁻¹ appeared (the first one ascribed to the C—O stretch vibration, or to the vibration of the COOH group in oleic acid [22,23], the second one to the C=O stretch vibration [14]).

The FT-IR spectra of Fe₃O₄ + CLA2 and Fe₃O₄-SiO₂ + CLA2 NPs are reported in Fig. 3. The silica presence is evidenced by: a new peak at about 1060 cm⁻¹, attributed to the asymmetric stretching of the Si—O—Si group, two peaks at 960 and 780 cm⁻¹, attributed Si—OH stretching vibration and Si—O—Si symmetric stretching [25,26], and a band at about 3000–3300 cm⁻¹, ascribable to OH groups. The peaks at 2852 e 2922 cm⁻¹ can be assigned respectively to the asymmetric and symmetric stretching of CH₂ group of CLA, the band at about 1500–1640 cm⁻¹, attributed to the asymmetric and symmetric stretch vibration of adsorbed COO⁻ group [14,22], and the peak at about 1408 cm⁻¹ ascribed to the “umbrella” bending mode of CH₃ group. Also in this samples the peak at about 1710 cm⁻¹, ascribable to the C=O vibration of CLA, appears.

Fig. 4 reports the behavior of the various NP suspensions after different times of sedimentation. The precipitation of Fe₃O₄ + CLA1 NPs starts after 5 min and is already complete after 30 min. The Fe₃O₄ + CLA2 and Fe₃O₄-SiO₂ + CLA2 solutions are both still stable after 2 h, and only Fe₃O₄-SiO₂ + CLA2 also after 24 h.

3.2. The effect of SPIONs and CLA alone on mouse breast cancer 4T1 cells and on mouse pancreatic islet endothelial MS1 cells

SPIONs, washed or not, and SPIONs functionalized with CLA (low and high amount, one- or two-steps) were tested to choose the preparation

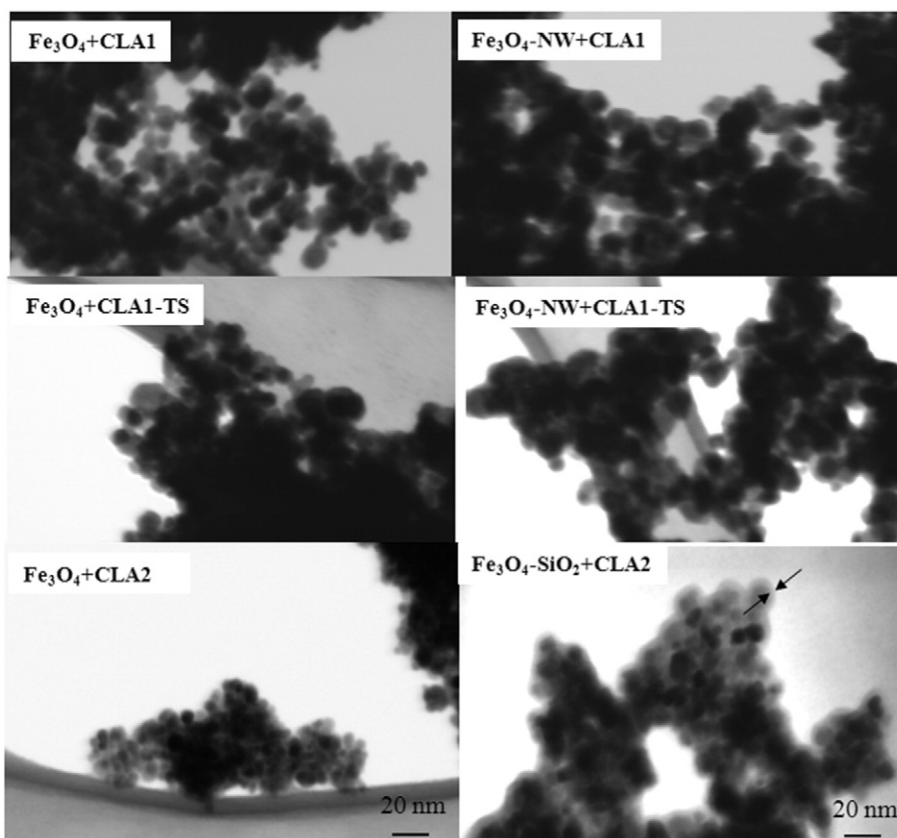


Fig. 1. STEM images of SPIONs. Fe_3O_4 + CLA1, washed CLA-capped Fe_3O_4 NPs; Fe_3O_4 -NW + CLA1, not washed CLA-capped Fe_3O_4 NPs; Fe_3O_4 + CLA1-TS, washed two step CLA-capped Fe_3O_4 NPs; Fe_3O_4 -NW + CLA1-TS NPs, not washed two step CLA-capped Fe_3O_4 NPs; Fe_3O_4 + CLA2; Fe_3O_4 - SiO_2 + CLA2, silica shell-coated, washed CLA-capped Fe_3O_4 NPs. CLA1, 3.0 μl of CLA/ml of NPs; CLA2, 4.5 μl of CLA/ml of NPs.

showing the highest inhibition of 4T1 cell proliferation. All functionalized particles decrease cell number in comparison with SPIONs not functionalized with CLA (Fe_3O_4), being the major inhibition obtained by SPIONs washed and capped with CLA with one-step procedure (data not

shown). Therefore, in the following experiments, only Fe_3O_4 , Fe_3O_4 + CLA1 and Fe_3O_4 + CLA2, with or without silica shell, were compared.

Fig. 5 shows the percentages of viability in cells treated with various SPIONs in comparison with the control cells, set to 100%. The viability in

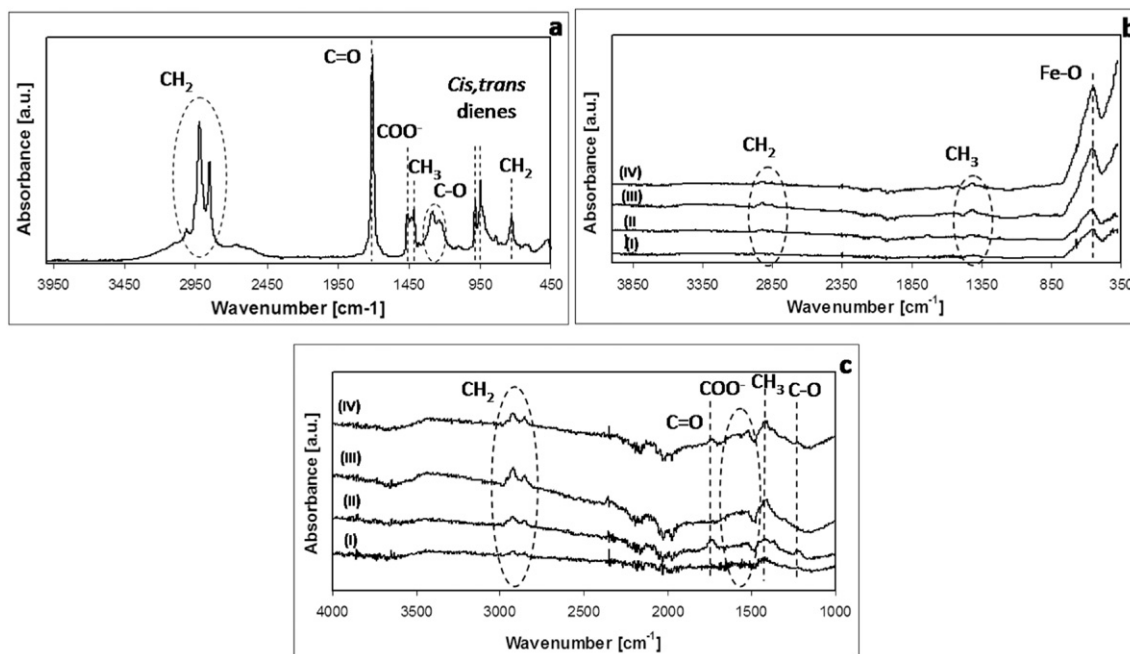


Fig. 2. FT-IR spectra. (a) FT-IR spectra of pure CLA; (b) whole spectrum of Fe_3O_4 -NW + CLA1 (curve I), Fe_3O_4 -NW + CLA1-TS (curve II), Fe_3O_4 + CLA1 (curve III), Fe_3O_4 + CLA1-TS (curve IV) NPs; (c) selected windows between 1000 and 4000 cm^{-1} . See legend in **Fig. 1** for NP acronyms.

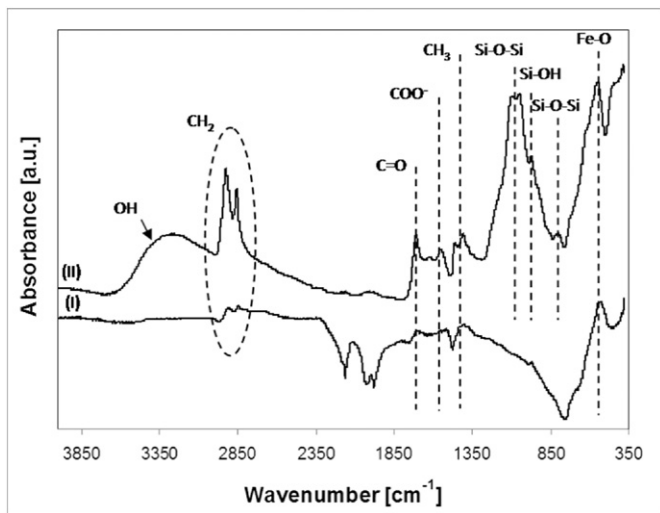


Fig. 3. FT-IR spectra. FT-IR spectra of Fe_3O_4 + CLA2 (curve I) and $\text{Fe}_3\text{O}_4\text{-SiO}_2$ + CLA2 (curve II) NPs. See legend in Fig. 1 for NP acronyms.

cells treated with Fe_3O_4 + CLA1, Fe_3O_4 + CLA2 or $\text{Fe}_3\text{O}_4\text{-SiO}_2$ + CLA2 is lower than in control cells and in cells treated with Fe_3O_4 and $\text{Fe}_3\text{O}_4\text{-SiO}_2$.

When the cells were treated with SPIONs coated or not with silica and capped or not with CLA, the reduction of viability is higher in cells treated with Fe_3O_4 + CLA2 than in the cells treated with other ones. No significant difference was found between 48 and 72 h for cells treated with SPIONs + CLA for both quantity of NPs. The NP internalization by cells was evidenced with iron staining (Fig. 6). NPs functionalized or not with CLA are present in the cells, whereas no staining is evident in cells untreated with NPs. The analysis by gas chromatography-mass

spectrometry of lipids extracted from 4T1 cells incubated with SPIONs coated or not with silica and capped or not with CLA shows that CLA is incorporated in lipids, and it is higher in cells treated with Fe_3O_4 + CLA2 in comparison with cells treated with Fe_3O_4 + CLA1 NPs (Table 2). With regards the incorporation of CLA in lipids extracted from 4T1 cells incubated with $\text{Fe}_3\text{O}_4\text{-SiO}_2$ + CLA2, the Table 2 showed a lesser incorporation of CLA for isomer 1 and 2 and a slight increase for the isomer 3.

The effect of CLA alone on 4T1 cell viability is reported in Table 3. Two concentrations of CLA similar to the quantity used for the preparation of SPIONs were added to the 4T1 cells. A time-dependent reduction of cell viability was observed.

To verify whether the different types of SPIONs affected in different way normal and cancer cells, pancreatic islet endothelial MS1 cells were treated. For these experiments, only CLA2 (4.5 μl CLA/ml of NPs) was used. Table 4 shows that no decrease of viability was induced by all types of SPIONs in comparison with control cells. In particular there were no differences between SPIONs capped or not with CLA.

Fig. 7 reports that NPs coated or not with silica and capped or not with CLA are present in the MS1 cells.

Prussian blue staining was used to evidence the presence of SPIONs with and without silica capped or not with CLA in pancreatic islet endothelial MS1 cells. As shown in the panels, all the SPIONs highly interact with MS1 cells, with the exception of silica coated with CLA, that are less internalized in cells. It was reported only the iron staining relative to 16 $\mu\text{g}/100,000$ cells of various SPIONs after 24 h of treatment. See Table 1 for NP acronyms.

4. Discussion

In recent years, NPs have been proposed for biomedical utilization [27–31]. This approach implies the synthesis of biocompatible NPs, which are also stable and easily manageable in biological media. For

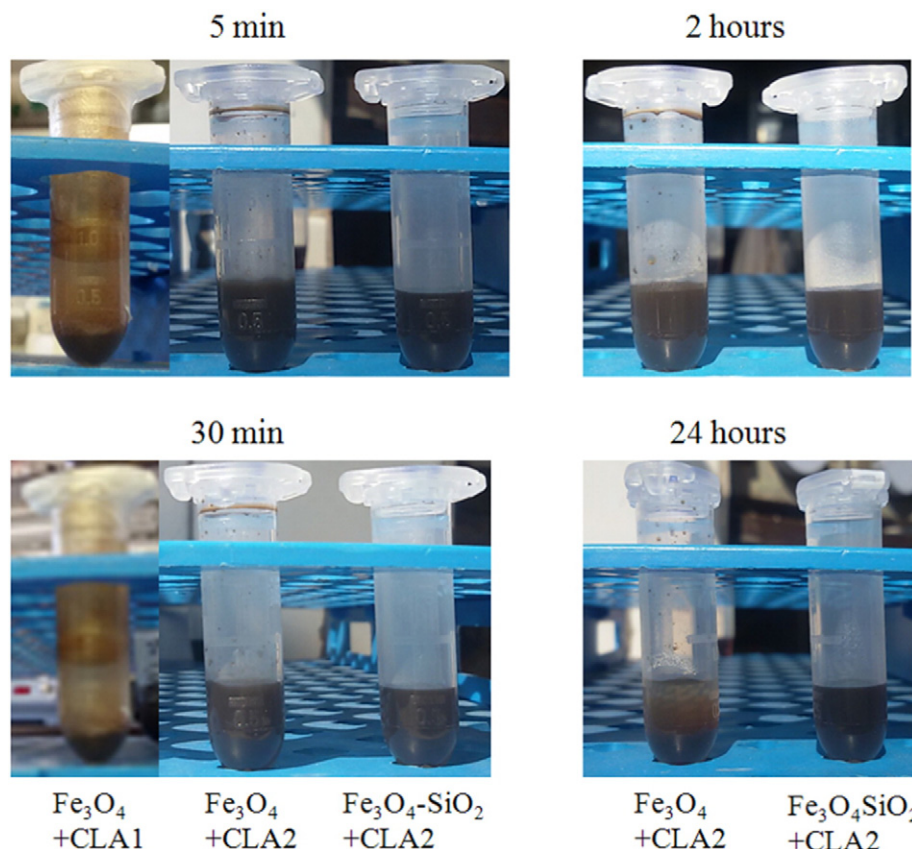


Fig. 4. Precipitation of SPIONs. Time of precipitation of NPs with or without silica, capped or not with CLA. See Table 1 for NPs acronyms.

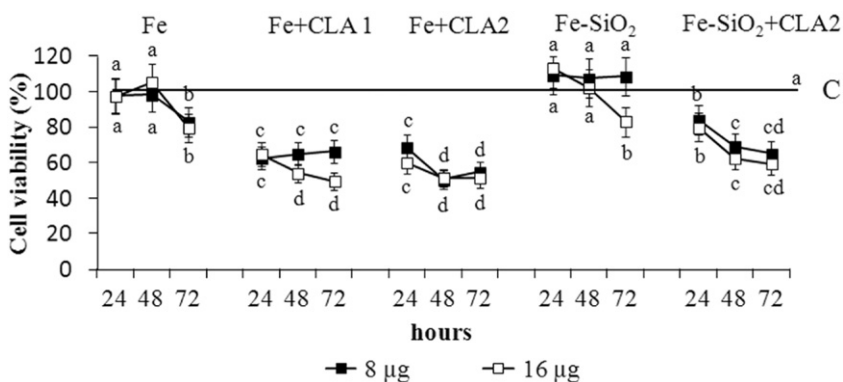


Fig. 5. Viability of mouse breast cancer 4T1 cells exposed to Fe_3O_4 NPs coated or not with silica and capped or not with CLA. The values are means \pm S.D. of 4 experiments and are expressed as % of control cells set equal to 100%. The absorbance values of control are 0.591 ± 0.192 for 24 h, 1.457 ± 0.151 for 48 h and 1.596 ± 0.168 for 72 h. For each NP quantity (8 or 16 μg), means with different letters are significantly different from one another ($p < 0.05$) as determined by analysis of variance followed by a post-hoc Newman-Keuls test. See Table 1 for NPs acronyms. C, control cells (black line); 8 μg , 16 μg , were the quantity of various NPs added to 100,000 cells.

this reason, several coatings have been proposed to improve colloidal stability, prevent oxidation, and improve biocompatibility of NPs [10]. Among them, fatty acids have been also investigated.

Some authors have used OA, which belongs to unsaturated monocarboxylic acids, to functionalize Fe_3O_4 NPs; in particular the study reported by Hemei Chen et al. [32] showed that OA capped Fe_3O_4 NPs possessed high magnetization and were useful to further adsorb other biomacromolecules. Other studies, instead of using a single adsorption layer of OA, stabilized magnetic NPs by short-chain-length monocarboxylic acids, such as lauric acid and myristic acid [33], but the magnetic NPs were in part aggregated [34]. However, magnetic NPs coated with myristic or lauric acids were cytotoxic for glioblastoma cells, showing low toxicity for normal astrocytes [33]. Starting from the evidence that fatty acids seem biocompatible for healthy cells and toxic for cancer cells, the rationale of their use as capping agent for magnetic NPs should be adjusted, trying to optimize their role as NPs driven therapeutic agents, not only as biocompatible surfactants.

In this study, CLA was chosen as capping agent for magnetic NPs for its antitumor properties [11–13]; its effect on colloidal stability of NPs suspensions and its potential therapeutic effect, when grafted on NPs, were evaluated. The effect of silica coating was also investigated. The superparamagnetic properties of pure Fe_3O_4 NPs were previously assessed [21]. The size and morphology of the NP batch prepared for this research were investigated and a good reproducibility of the results was observed in respect of previous preparations, both for uncoated and silica coated magnetic NPs. The presence of CLA on the magnetic NPs was evidenced by the FT-IR analysis. The results showed the presence of iron oxide and of organic species ascribable to CLA on all samples. It can therefore be assumed that all the functionalization methods were successful. Interestingly it can be evidenced that different signals ascribable to CLA, which could be related to the presence of a single- or bi-layered configuration, were present. All functionalized particles showed the signals related to the CLA main chain (2852 e 2922 cm^{-1} of CH_2 group and 1408 cm^{-1} of CH_3 group [14]). Moreover, in all functionalized NPs also the band ascribed to asymmetric and symmetric stretch

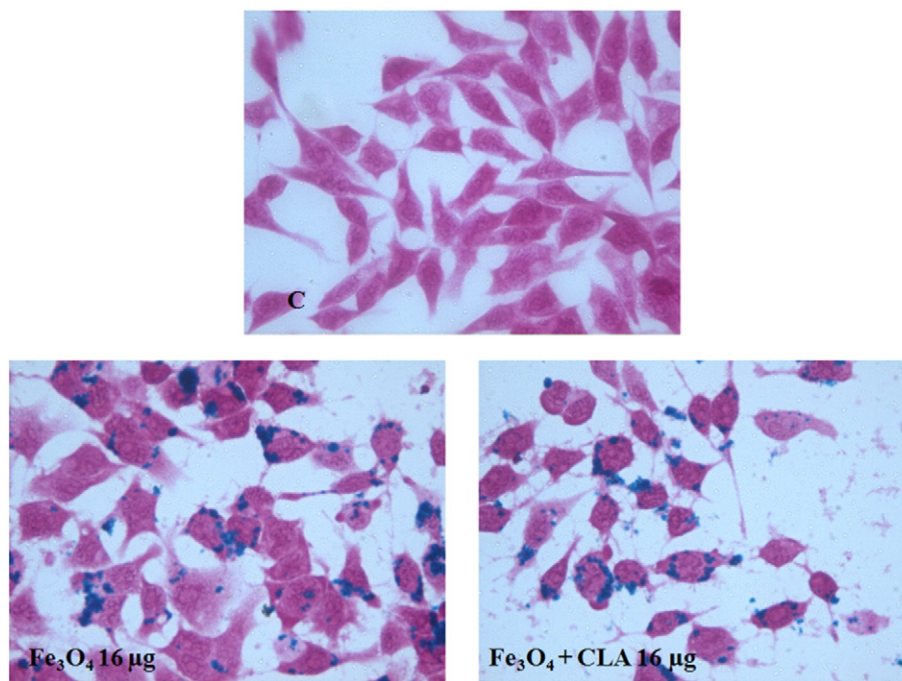


Fig. 6. Iron staining. Prussian blue staining was used to evidence the presence of SPIONs with and without silica capped or not with CLA in the mouse breast cancer 4T1 cells. It was reported only the iron staining relative to 16 μg /100,000 cells of various SPIONs after 72 h of treatment. C, control cells without SPIONs; see Table 1 for NPs acronyms.

Table 2

Conjugated linoleic acid (CLA) in lipids extracted from 4T1 cells treated for 72 h with SPIONs coated or not with silica and capped or not with CLA. The values are means of two experiments and are expressed as number of times the control cells (C) set equal to 1. See legend in Table 1 for NPs acronyms. 16 μg were the quantity of NPs added to 100,000 cells.

Sample	CLA: 3 isomers		
	Isomer n. 1	Isomer n. 2	Isomer n. 3
C	1	1	1
Fe ₃ O ₄ 16 μg	0.90	0.72	0.68
Fe ₃ O ₄ + CLA1 16 μg	1.97	15.30	1.08
Fe ₃ O ₄ + CLA2 16 μg	2.75	19.70	1.26
Fe ₃ O ₄ -SiO ₂ + CLA2 16 μg	1.52	1.64	1.61

vibration of COO⁻ group (1500–1640 cm⁻¹) appeared [14,22]. This band was not present in the FT-IR spectrum of pure CLA (i.e. not adsorbed on any support) since it can be related to the covalent interaction between COO⁻ groups and Fe atoms in a chelating bidentate interaction with iron oxide surfaces [22]. The patterns of the Fe₃O₄ + CLA1-TS and Fe₃O₄-NW + CLA1-TS revealed signals also present in not adsorbed CLA (1250–1285 cm⁻¹ for C=O [22,23] and 1710 cm⁻¹ C=O [14]), but absent in the patterns of CLA adsorbed on NPs with a single-step procedure and low CLA content (see for example the patterns of Fe₃O₄ + CLA1, Fe₃O₄-NW + CLA1 and [23]), as a demonstration of the presence of free —COOH groups exposed on the NP surface, typical of a bi-layer configuration [14]. The functionalization with highest CLA amount, even in a single step (Fe₃O₄ + CLA2 and Fe₃O₄-SiO₂ + CLA2), gave FT-IR results similar to Fe₃O₄ + CLA1-TS and Fe₃O₄-NW + CLA1-TS NPs both with and without the presence of silica shell. In this case the excess of CLA probably produced a secondary layer, with a configuration similar to the one obtained by the two-step synthesis procedure [14].

The NPs functionalized with CLA in a one step were chosen, among different preparations of SPIONs, because they reduced cell viability more than NPs coated with CLA with two-step procedure (data not shown). Two amounts of CLA (one step) were used: Fe₃O₄ + CLA1 (3 μl CLA/ml of NPs) and Fe₃O₄ + CLA2 (4.5 μl of CLA/ml of NPs). The results obtained showed that both Fe₃O₄ + CLA1 and Fe₃O₄ + CLA2 reduced the cell viability of 4 T1 cells treated for 24 and 72 h, respect to control cells not incubated with SPIONs and to 4 T1 cells incubated with SPIONs without CLA, but Fe₃O₄ + CLA2 was more effective in the reduction than Fe₃O₄ + CLA1. For Fe₃O₄ + CLA2, the viability values were not significantly different between 48 and 72 h. A similar trend was observed in 4 T1 cells treated with CLA alone.

To be highlighted that the experiments, carried out to evaluate the effect of various SPIONs on normal cells, showed that SPIONs capped or not with CLA2 and coated or not with silica did not decrease the viability of the normal MS1 cells.

The NP precipitation time with both CLA amounts was also determined. Although all the particles seem aggregated in STEM images of Fig. 1 suspensions stable up to 24 h were obtained (Fig. 4), as discussed below. This observation may be explained by the fact that STEM images of the particles were obtained after drying a drop (5 μl) of the suspension onto a carbon coated copper TEM grid. Upon drying onto a

Table 3

Viability of mouse breast cancer 4T1 cells exposed to CLA.

Sample	24 h	48 h	72 h
C	100	100	100
CLA 10 μM	91.7	69.1	72.0
CLA 25 μM	86.5	69.2	69.5

The values are means of 2 experiments and are expressed as % of control cells set equal to 100%. The absorbance values of control are 0.591 \pm 0.192 for 24 h, 1.457 \pm 0.151 for 48 h and 1.596 \pm 0.168 for 72 h. C, control cells.

Table 4

Viability of pancreatic islet endothelial MS1 cells exposed to Fe₃O₄ NPs coated or not with silica and capped or not with CLA. The values are means of 2 experiments and are expressed as % of control cells set equal to 100%. The absorbance values of control are 0.256 for 24 h, 0.771 for 48 h and 0.601 for 72 h.

Sample	24 h		48 h		72 h	
	8 μg	16 μg	8 μg	16 μg	8 μg	16 μg
C	100	100	100	100	100	100
Fe ₃ O ₄	97.09	103.41	111.47	103.24	151.99	140.76
Fe ₃ O ₄ + CLA2	94.80	104.86	125.76	103.63	146.53	133.11
Fe ₃ O ₄ -SiO ₂	101.56	110.86	114.02	107.13	127.03	131.44
Fe ₃ O ₄ -SiO ₂ + CLA2	102.94	114.79	118.96	94.16	136.76	148.91

See Table 1 for NPs acronyms. C, control cells; 8 μg , 16 μg , were the quantity of various NPs added to 100,000 cells.

substrate particles obviously aggregates and appear as agglomerates in the images.

As shown in Fig. 4 the precipitation time was shorter for Fe₃O₄ + CLA1 than for Fe₃O₄ + CLA2: at 30 min Fe₃O₄ + CLA1 NPs were all precipitated, while Fe₃O₄ + CLA2 NPs remained in suspension up to 2 h. This difference can be explained taking into account that Fe₃O₄ + CLA2, even if synthesized with one step procedure, were covered by a secondary layer of CLA (see FT-IR results). It can be supposed that the highest amount of CLA caused a condition similar to that of bilayer-coated NPs (even if the bilayer was probably not continuous). It is reasonable that Fe₃O₄ + CLA2 NP surface is more hydrophilic in comparison to that of Fe₃O₄ + CLA1 ones (which do not expose free —COOH groups) and, in turn, NPs show a better stability in aqueous medium.

The determination, by gas chromatography-mass spectrophotometry, of CLA isomers in the lipids extracted from cells incubated with SPIONs functionalized or not with CLA, showed that this fatty acid was more incorporated in the cells treated with Fe₃O₄ + CLA2 NPs than in the cells treated with Fe₃O₄ + CLA1 NPs. The results of this study indicate that the use of the highest amount of CLA (4.5 μl /1 ml of NPs) improves the suspension stability, the CLA incorporation into the cells and the antitumor activity. It worth of mentioning that it is very important to avoid the formation of clusters, because they partially lose the magnetic properties, and, when injected intravascularly, show a shorter circulation time due to rapid clearance by monocytes, this decreasing the reaching of target cells or tissues.

Interestingly the NPs coated with a thin layer of silica and functionalized with CLA showed a further increase of time required to have the precipitation, in fact at 24 h Fe₃O₄-SiO₂ + CLA2 NPs were all dispersed in solution. This effect can be mainly attributed to the citric acid functionalization needed for silica coating, and cannot be ascribed exclusively to CLA amount. Fe₃O₄-SiO₂ + CLA2 NPs also cause a reduction of cell viability in comparison with control cells and CLA-free Fe₃O₄-SiO₂, but the inhibition was lower than that obtained with Fe₃O₄ + CLA2. In the same way, the incorporation of CLA in lipid extracted from the cells treated with Fe₃O₄-SiO₂ + CLA2 NPs was lower for the isomers 1 and 2 than that obtained with Fe₃O₄ + CLA2.

This difference could be ascribed to the role of the silica shell avoiding the direct contact between the magnetite NPs and the biological environment, which in turn reduces their potential toxicity.

Moreover, according to the reported data, we can infer that fatty acids may improve the affinity between NPs and cell membrane and favor particle internalization in tumor cells. This is an important issue for future research, for example for studies with other cancer cell lines as well as for magnetic NP-assisted gene therapy, to improve the use of viral vectors to transfer therapeutic genes to target cells [35–37].

5. Conclusions

In this research colloidal suspensions of Fe₃O₄ NPs, both uncoated or coated by silica shell, of about 5–20 nm in diameter, were successfully prepared and functionalized with different amounts of CLA both in

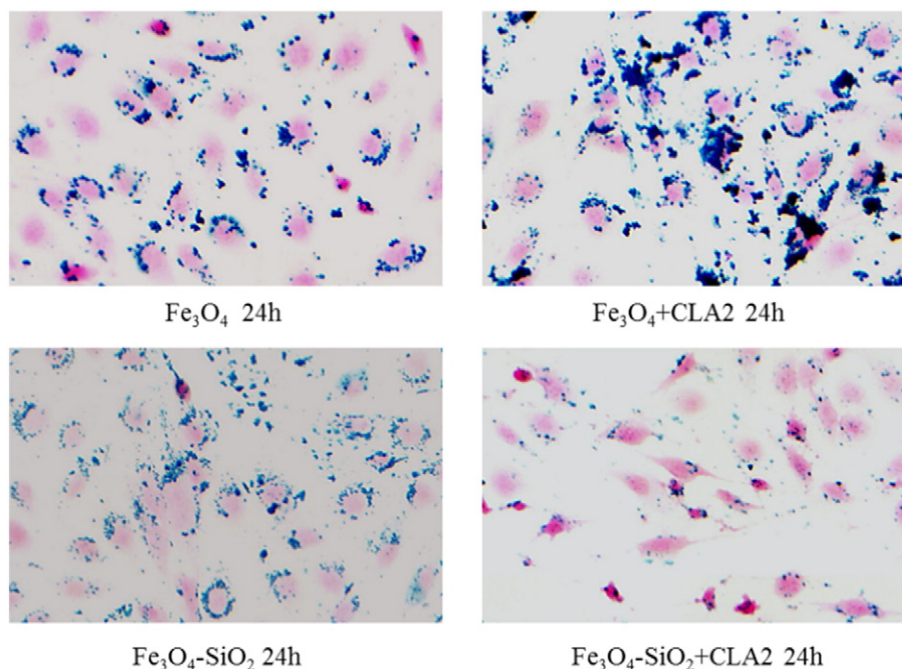


Fig. 7. Iron staining for MS1 cells.

single- and bi-layer configurations. Both the silica shell and CLA layer played a role in determining suspension stability, especially when CLA was grafted on the NP surface in a bi-layer configuration. The results evidenced that the viability of mouse breast cancer 4T1 cells was reduced in presence of Fe_3O_4 NPs functionalized with CLA in comparison with both untreated control cells and cells treated with CLA-free NPs. The presence of the silica coating in CLA capped NPs caused a lesser inhibition of cell viability. Since it is known that the colloidal stability must be assured to avoid uncontrolled NPs clusterization, loosening of magnetic properties and short circulation time, control of this parameter is crucial, even if it is not directly related to the antitumoral effect observed in this work. Based on these results, silica shell free Fe_3O_4 NPs functionalized with high amount of CLA (with bi-layered configuration) can be suggested as therapeutic carriers for their good dispersion and ability to decrease mouse breast cancer 4T1 cell viability.

Acknowledgments

This work was supported by grants from AIRC, Italy: (IG n. 13166), “Development of engineered magnetic nanoparticles for cancer therapy”, <http://www.airc.it> to A.F., from Compagnia di San Paolo (CSP-Torino-Piemonte: 12-CSP-C04-018), Italy to AF, and from the University of Turin (Local Research Funding ex-60%), Italy to RAC.

References

- [1] G. Kandasamy, D. Maity, Recent advances in superparamagnetic iron oxide nanoparticles (SPIONs) for in vitro and in vivo cancer nanotheranostics, *Int. J. Pharm.* 496 (2015) 191–218.
- [2] A. Schroeder, M.M. Winslow, J.E. Dahlman, G.W. Pratt, R. Langer, T. Jacks, D.G. Anderson, Treating metastatic cancer with nanotechnology, *Nat. Rev. Cancer* 12 (2012) 39–50.
- [3] S. Pietronave, D. Locarno, L. Rimondini, M. Prat, Functionalized nanomaterials for diagnosis and therapy of cancer, *J. Appl. Biomater. Biomech.* 7 (2009) 77–89.
- [4] B.J. Tefft, S. Uthamaraj, J.J. Harburn, M. Klabusay, D. Dragomir-Daescu, G.S. Sandhu, Cell labeling and targeting with superparamagnetic iron oxide nanoparticles, *J. Vis. Exp.* (2015) <http://dx.doi.org/10.3791/53099>.
- [5] B.D. Brown, L. Naldini, Exploiting and antagonizing microRNA regulation for therapeutic and experimental applications, *Nat. Rev. Genet.* 10 (2009) 578–585.
- [6] D. Maity, P. Chandrasekharan, P. Pradhan, K.H. Chuang, J.M. Xue, S.S. Feng, J. Ding, Novel synthesis of superparamagnetic magnetite nanoclusters for biomedical applications, *J. Mater. Chem.* 21 (2011) 14717–14724.
- [7] J. Majeed, L. Pradhan, R.S. Ningthoujam, R.K. Vatsa, D. Bahadur, A.K. Tyagi, Enhanced specific absorption rate in silanol functionalized Fe_3O_4 core-shell nanoparticles: study of Fe leaching in Fe_3O_4 and hyperthermia in L929 and HeLa cells, *Colloids Surf. B: Biointerfaces* 122 (2014) 396–403.
- [8] N. Landázuri, S. Tong, J. Suo, G. Joseph, D. Weiss, D.J. Sutcliffe, D.P. Giddens, G. Bao, W.R. Taylor, Magnetic targeting of human mesenchymal stem cells with internalized superparamagnetic iron oxide nanoparticles, *Small* 9 (2013) 4017–4026.
- [9] J. Park, K. An, Y. Hwang, J.G. Park, H.J. Noh, J.Y. Kim, J.H. Park, N.M. Hwang, T. Hyeon, Ultra-large-scale syntheses of monodisperse nanocrystals, *Nat. Mater.* 3 (2004) 891–895.
- [10] W. Wu, Z. Wu, T. Yu, C. Jiang, W.S. Kim, Recent progress on magnetic iron oxide nanoparticles: synthesis, surface functional strategies and biomedical applications, *Sci. Technol. Adv. Mater.* 16 (2015) 023501.
- [11] M.A. Belury, Inhibition of carcinogenesis by conjugated linoleic acid: potential mechanisms of action, *J. Nutr.* 132 (2002) 2995–2998.
- [12] M. Maggiora, et al., An overview of the effect of linoleic and conjugated-linoleic acids on the growth of several human tumor cell lines, *Int. J. Cancer* 112 (2004) 909–919.
- [13] G. Muzio, M. Oraldi, A. Trombetta, R.A. Canuto, PARalpha and PP2A are involved in the proapoptotic effect of conjugated linoleic acid on human hepatoma cell line SK-HEP-1, *Int. J. Cancer* 121 (2007) 2395–2401.
- [14] K. Yang, H. Peng, Y. Wen, N. Li, Re-examination of characteristic FTIR spectrum of secondary layer in bilayer oleic acid coated Fe_3O_4 nanoparticles, *Appl. Surf. Sci.* 256 (2010) 3093–3097.
- [15] S. Campelj, D. Makovec, M. Drogenik, Preparation and properties of water-based magnetic fluids, *J. Phys. Condens. Matter* 20 (2008) 204101 (5pp) 10.1088/0953-8984/20/20/204101.
- [16] W. Stöber, A. Fink, Controlled growth of monodisperse silica spheres in the micron size range, *J. Colloid Interface Sci.* 26 (1968) 62–69.
- [17] J. Folch, M. Lees, G.H. Sloane Stanley, A simple method for the isolation and purification of total lipides from animal tissues, *J. Biol. Chem.* 226 (1957) 497–509.
- [18] S. Klem, M. Klinger, H. Demmelmair, B. Koletzko, Efficient and specific analysis of red blood cell glycerophospholipid fatty acid composition, *PLoS One* 7 (2012) e33874.
- [19] T.Y. Yen, B. Stephen Inbaraj, J.T. Chien, B.H. Chen, Determination of conjugated linoleic acids and cholesterol oxides and their stability in a model system, *Anal. Biochem.* 400 (2010) 130–138.
- [20] N. Sánchez-Ávila, J.M. Mata-Granados, J. Ruiz-Jiménez, M.D. Luque de Castro, Fast, sensitive and highly discriminant gas chromatography–mass spectrometry method for profiling analysis of fatty acids in serum, *J. Chromatogr. A* 1216 (2009) 6864–6872.
- [21] E. Verné, et al., Iron-oxide nanoparticles used for target cancer gene therapy and hyperthermia, Proceedings of the 29th Annual Meeting of the European Society for Hyperthermic Oncology, 56, Minerva Med 2014, p. 16.
- [22] L. Zhang, R. He, H.C. Gu, Oleic acid coating on the monodisperse magnetite nanoparticles, *Appl. Surf. Sci.* 253 (2006) 2611–2617.
- [23] V.V. Korolev, A.G. Ramazanova, A.V. Blinov, Adsorption of surfactants on superfine magnetite, *Russ. Chem. Bull.* 51 (2002) 2044–2049 (Int. Ed.).
- [24] J.V. Kadamne, C.L. Castrodale, A. Proctor, Measurement of Conjugated Linoleic Acid (CLA) in CLA-Rich Potato Chips by ATR-FTIR Spectroscopy, *J. Agric. Food Chem.* 59 (2011) 2190–2196.

- [25] B. Mojic, K.P. Giannakopoulos, Z. Cvejic, V.V. Srdic, Silica coated ferrite nanoparticles: influence of citrate functionalization procedure on final particle morphology, *Ceram. Int.* 38 (2012) 6635–6641.
- [26] A. Fatemeh, H. Ali, N. Sirous, Surface modification of Fe₃O₄@SiO₂ microsphere by silane coupling agent, *Int. Nano Lett.* 3 (2013) 23.
- [27] S. Mornet, S. Vasseur, F. Grasset, P. Veverka, G. Goglio, A. Demourgues, J. Portier, E. Pollert, E. Duguet, Magnetic nanoparticles design for medical applications, *Prog. Solid State Chem.* 34 (2006) 237–247.
- [28] S.C. Wuang, K.G. Neoh, E.T. Kang, D.W. Pack, D.E. Leckband, Heparinized magnetic nanoparticles: in-vitro assessment for biomedical applications, *Adv. Funct. Mater.* 16 (2006) 1723–1730.
- [29] E. Duguet, S. Vasseur, S. Mornet, J.M. Devoisselle, Magnetic nanoparticles and their applications in medicine, *Nanomedicine* 1 (2006) 157–168.
- [30] J.P. Fortin, C. Wilhelm, J. Servais, C. Ménager, J.C. Bacri, F. Gazeau, Size-sorted anionic iron oxide Nanomagnets as colloidal mediators for magnetic hyperthermia, *J. Am. Chem. Soc.* 129 (2007) 2628–2635.
- [31] N.A. Brusentsov, L.V. Nikitin, T.N. Brusentsova, A.A. Kuznetsov, F.S. Bayburtskiy, L.I. Shumakov, N.Y. Jurchenko, Magnetic field hyperthermia of the mouse experimental tumor, *J. Magn. Mater.* 252 (2002) 378–380.
- [32] H. Chen, S. Liu, Y. Li, C. Deng, X. Zhang, P. Yang, Development of oleic acid-functionalized magnetite nanoparticles as hydrophobic probes for concentrating peptides with MALDI-TOF-MS analysis, *Proteomics* 11 (2011) 890–897.
- [33] M.V. Avdeev, K. Lamszus, L. Vekas, V.M. Garamus, A.V. Feoktystov, O. Marinica, R. Turcu, R. Willumeit, Structure and in vitro biological testing of water-based ferrofluids stabilized by monocarboxylic acids, *Langmuir* 26 (2010) 8503–8509.
- [34] D. Bica, L. Vekas, M.V. Avdeev, O. Marinic, V. Socoliuc, M. Balasoiu, V.M. Garamus, Sterically stabilized water based magnetic fluids: synthesis, structure and properties, *J. Magn. Mater.* 311 (2007) 17–21.
- [35] M. Wiznerowicz, T.D. Harnessing, HIV for therapy, basic research and biotechnology, *Trends Biotechnol.* 23 (2005) 42–47.
- [36] A. Follenzi, L.E. Ailles, S. Bakovic, M. Geuna, L. Naldini, Gene transfer by lentiviral vectors is limited by nuclear translocation and rescued by HIV-1 pol sequences, *Nat. Genet.* 25 (2000) 217–222.
- [37] A. Follenzi, L. Naldini, HIV-based vectors. Preparation and use, *Methods Mol. Med.* 69 (2002) 259–274.